Polar Record 31 (177): 115–128 (1995). Printed in Great Britain.

Ice processes and growth history on Arctic and sub-Arctic lakes using ERS-1 SAR data

K. Morris, M.O. Jeffries, and W.F. Weeks
Geophysical Institute, University of Alaska, PO Box 757320, Fairbanks, AK 99775-7320, USA

Received June 1994

ABSTRACT. A survey of ice growth and decay processes on a selection of shallow and deep sub-Arctic and Arctic lakes was conducted using radiometrically calibrated ERS-1 SAR images. Time series of radar backscatter data were compiled for selected sites on the lakes during the period of ice cover (September to June) for the years 1991–92 and 1992–93. A variety of lake-ice processes could be observed, and significant changes in backscatter occurred from the time of initial ice formation in autumn until the onset of the spring thaw. Backscatter also varied according to the location and depth of the lakes. The spatial and temporal changes in backscatter were most constant and predictable at the shallow lakes on the North Slope of Alaska. As a consequence, they represent the most promising sites for long-term monitoring and the detection of changes related to global warming and its effects on the polar regions.

Contents

Introduction

Lakes represent an important natural resource in the Arctic. Many communities depend on lakes that do not freeze completely to the bottom for their fresh-water supply during the winter. These lakes also provide a habitat in winter for animal life. Consequently, the ability to monitor the freeze-up and break-up dates of lakes — that is, the duration of the ice-covered season — and to determine which lakes do not freeze to the bottom in the winter is very important for wildlife and water resources management. In recent decades, some areas of the Arctic have experienced a climate warming (for example, Chapman and Walsh 1993), and numerical climate models suggest that the effects of global warming will be experienced first and will be amplified in the polar regions (for example, Manabe and others 1992). There is evidence that the duration of the lake-ice cover is closely related to climate variability, and that changes in the length of the ice-covered season could have significant consequences for lake hydrology and biology (Palecki and others 1985; Palecki and Barry 1986; Schindler and others 1990). Since the timing of lake freeze-up and break-up is primarily a function of air temperature variations, the availability of a long-term record of these lake-ice benchmarks could contribute to the identification of the onset and subsequent effects of climate change at high latitudes.

Remote sensing provides the most practical method for long-term continuous monitoring and study of polar lakes. Much of the present understanding of high-latitude lake-ice properties and processes by remote-sensing methods is the result of studies of ice on shallow lakes on the North Slope of Alaska. Since the early 1970s, they have been studied occasionally, and primarily in late winter, using airborne X- and L-band real aperture radars in combination with surface observations and measurements (Sellmann and others 1975a, 1975b; Elachi and others 1976; Weeks and others 1977, 1978, 1981). Only one time series of radar images of lake-ice development in this region was compiled (Mellor 1982). This early research identified some of the factors that affected backscatter and showed that it was possible to differentiate between floating ice and ice that was frozen to the lake bottom, and thus make inferences about water depth. Unfortunately, those studies relied on uncalibrated photographic products and the analysis was qualitative. Recently, radiometrically calibrated, geolocated European Remote Sensing Satellite-1 (ERS-1) synthetic aperture radar (SAR) data (C-band), available in digital form from the Alaska SAR Facility, have been combined with field observations and modelling in more quantitative studies of backscatter variations in relation to ice-growth processes and structure throughout the ice-growth season on shallow North Slope lakes (Jeffries and others 1993, 1994; Wakayabashi and others 1993a, 1993b).

Because spaceborne SARs such as ERS-1 can obtain images of the polar regions regardless of light and cloud conditions, and because the data are available as geolocated and radiometrically calibrated digital products, they offer previously unavailable opportunities for quantitative studies of lake-ice growth processes and history throughout the winter. In order to realise the full potential of SAR for studies of high-latitude lake ice in relation to climate change, and wildlife and water resources management, it is important to understand the lake-ice growth processes and history that are being observed by these instruments. This paper presents further results from the study of the shallow, Alaskan North Slope lakes, and broadens the scope of lake-ice investigations using SAR to include deep and shallow Arctic and sub-Arctic lakes. Lake-ice backscatter variations observed in ERS-1 images and their relationship to factors such as ice growth, thickening and freezing to the bottom, the development of air inclusions in the ice, ice deformation, and the effects of precipitation

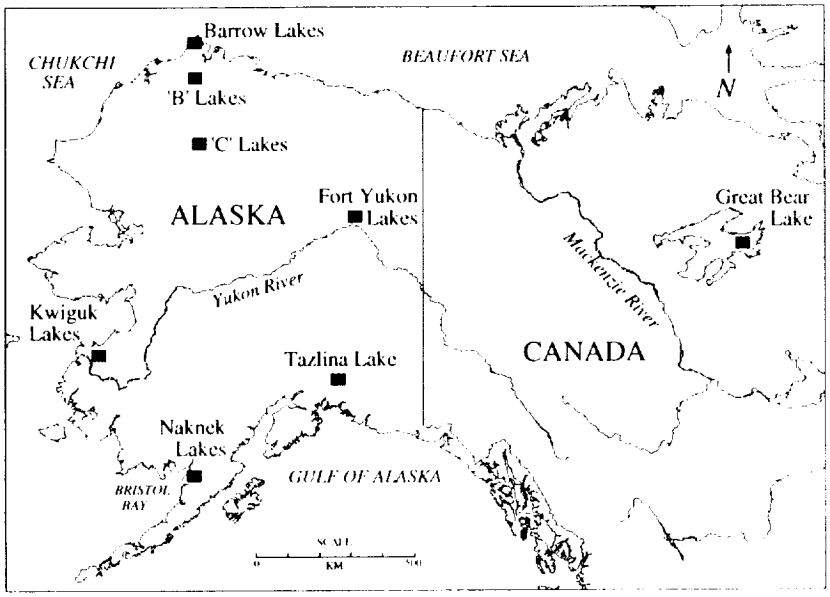

Fig. 1. Map showing the location of individual lakes or groups of lakes investigated in the study.

and air temperature changes on the snow and ice surface are discussed.

Study lakes and methods

The locations of the lakes chosen for this study are shown in Figure 1. The lakes include:

1. small, shallow (many <2 m deep) Arctic lakes located on the North Slope of Alaska (Barrow lakes at 71°13'5"N, 156°39'W; 'B' lakes at 70°22'5"N, 156°30'W, and 'C' lakes at 68°45'39"N, 156°15'W) and in the interior of Alaska near Fort Yukon (66°45'N, 145°30'W);
2. two groups of sub-Arctic lakes (Kwiguk lakes in the Yukon delta at 62°40'N, 163°20'W, and the Naknek lakes near Bristol Bay at 58°37'N, 157°W); and
3. two deep-water lakes, one sub-Arctic (Tazlina Lake at 61°52'N, 146°45'W) and one Arctic (Great Bear Lake at 66°5'N, 119°W).

A total of 233 ASF Standard low-resolution ERS-1 SAR images obtained from the Alaska SAR Facility were used for this study. These images cover a ground area of 100 km by 100 km and have a spatial resolution of 240 m and a pixel size of 100 m. Acquisition times for the images cluster around midday and midnight local time. For the quantitative analysis of backscatter variability within a single scene and between multiple scenes, these data were converted from DN values to radiometrically calibrated σ^o values using MacSigma-0 public-domain software developed at the Jet Propulsion Laboratory. Backscatter (σ^o) time series from September to June were created for selected sites on the lakes. The lakes to be studied were selected from an ERS-1 SAR scene of the area acquired in late winter 1992. Lakes that are in close proximity to each other and that have interesting and differing backscatter returns were chosen. In the case of the Barrow lakes, easy accessibility to the lakes from the town-site was also considered, as fieldwork would be performed on these lakes (Jeffries and others 1994). The latitude and longitude of each site in an ERS-1 SAR image were identified and the closest obtainable co-ordinates in all of the other images were sampled. Since the standard processed data are geometrically corrected with the restituted state vectors of the orbit, which introduces an error into the registration of the extracted coordinates, it was sometimes necessary to visually select the appropriate pixels for sampling. Because many of the lakes are quite small or have distinctive shorelines, this did not pose a serious problem. The σ^o value represents the mean of a nine-pixel square that has the site location as its center. The backscatter of undeformed ice adjacent to deformation features in the early stage of ice development was also determined at some lakes. When possible, that is, when sufficient data were available, time series for consecutive seasons (1991–92 and 1992–93) were compiled and compared. Data availability was primarily dependent on whether SAR data acquisition had been scheduled by the European Space Agency.

Weather records for the nearest meteorological station were obtained. In some cases, the records of several stations were consulted for a single group of lakes. This was necessary because the records for the closest station were incomplete or because there is no single station close to the desired lake location and its weather conditions had to be inferred from the records of several stations over a broad region. The weather records were used to investigate whether particular backscatter changes correlated with meteorological changes.

Background on lake-ice growth, structure, and backscatter

Much of the present knowledge of lake-ice growth, structure, and backscatter is based on investigations of ice on the shallow lakes of the North Slope of Alaska. This section summarizes the present state of knowledge and provides a basis for the interpretation of the SAR images of the lakes that were investigated in this study.

Lake ice is comprised primarily of congelation ice that is the product of downward growth of ice crystals into the water as heat is conducted through the ice from the growth interface to the atmosphere. This ice can be either clear or contain bubbles or both. Typically, the ice on the shallow lakes of the Alaskan North Slope has a bi-layer character, with a layer of clear ice, sometimes several decimeters in thickness, overlying a layer of ice containing tubular bubbles (Weeks and others, 1977, 1978, 1981; Mellor 1982; Jeffries and others 1993, 1994). The tubular bubbles

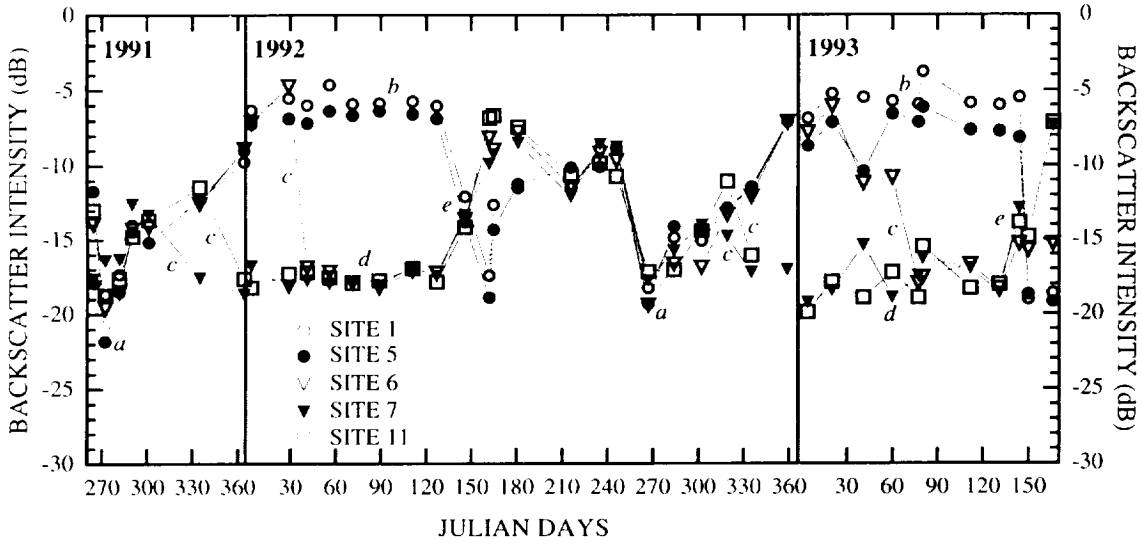

Fig. 2. Time series of backscatter intensity (σ°) for selected Barrow lakes from September 1991 to June 1993. Several recurring features are identified: (a) the onset of freezing at about Julian day 270; (b) the prolonged maxima from floating ice from mid-winter to spring; (c) the grounding of ice on the bottom of lakes; (d) the prolonged minima from grounded ice until spring; and (e) the onset of melting in May.

are oriented with their long axes parallel to the growth direction. The clear ice represents the earlier stages of ice growth when all gases are rejected back into the water during freezing, and the appearance of the tubular bubbles probably represents the time when these shallow reservoirs become supersaturated with gas (Jeffries and others 1994).

As long as the ice remains afloat, there will be specular reflection of the radar signal off the basal ice–water interface because of the strong dielectric contrast between the two media (Weeks and others 1978; Leconte and Klassen 1991). When there are few or no inclusions present, this specular reflection leads to most of the signal being reflected away from the radar and the ice appears relatively dark in a radar image. Ice that is frozen to the bottom of a lake also appears dark in SAR images because there is a low dielectric contrast between the ice and lake sediments and the signal is absorbed into the lake bottom; consequently, there is little or no return to the radar (Weeks and others 1977, 1978, 1981; Mellor 1982; Leconte and Klassen 1991; Jeffries and others 1993, 1994; Wakabayashi and others 1993b). It has been noted that, since tubular bubbles occur in both floating ice and grounded ice on the shallow North Slope lakes, the tubular bubbles must act as forward scatterers producing a strong return to the radar from floating ice and bright signatures in SAR images (Weeks and others 1977, 1978, 1981; Mellor 1982; Jeffries and others 1993, 1994).

After initial freeze-up, a layer of snow accumulates on the ice surface. The base of the snow can be flooded by water reaching the surface through cracks formed by thermal stresses or the weight of snow on the ice surface. Freezing of the wet snow forms snow-ice that contains many spherical bubbles. Jeffries and others (1994) suggested that the magnitude of the effect of the bubbly snow-ice on backscatter from the North Slope lake ice is unknown. On the other hand, Hall and others (1994) suggested that it may be an important source of backscatter from alpine lakes.

Shallow Arctic lakes

Backscatter time series were compiled for the period September 1991 to June 1993 for the North Slope lakes (Barrow, 'B', and 'C'), and for the period September 1991 to May 1992 for the Fort Yukon lakes. The Barrow lakes data are representative of all of these datasets; thus, the following discussion will focus primarily on the Barrow lakes with reference to the three other shallow Arctic lake data sets as necessary. The time series for the Barrow lakes is illustrated in Figure 2. A number of annually recurring features are:

1. a steady increase in backscatter from early autumn to early January;
2. a backscatter maximum that is attained at many lakes in early January and is maintained until April/May;
3. a backscatter decrease at a number of lakes at different times during the winter, with minimum backscatter levels maintained thereafter until April/May;
4. rapid backscatter changes in late April/early May; and
5. high backscatter at all lakes during the short summer.

These features also occur in the time series for 'B' lakes, 'C' lakes, and Fort Yukon lakes.

Initial ice formation and early stages of ice growth

During the short summer and immediately prior to freeze-up, radar returns from the Barrow lakes are high, probably due to strong backscatter from the typically wind-roughened water surfaces. The onset of freezing in mid- to late

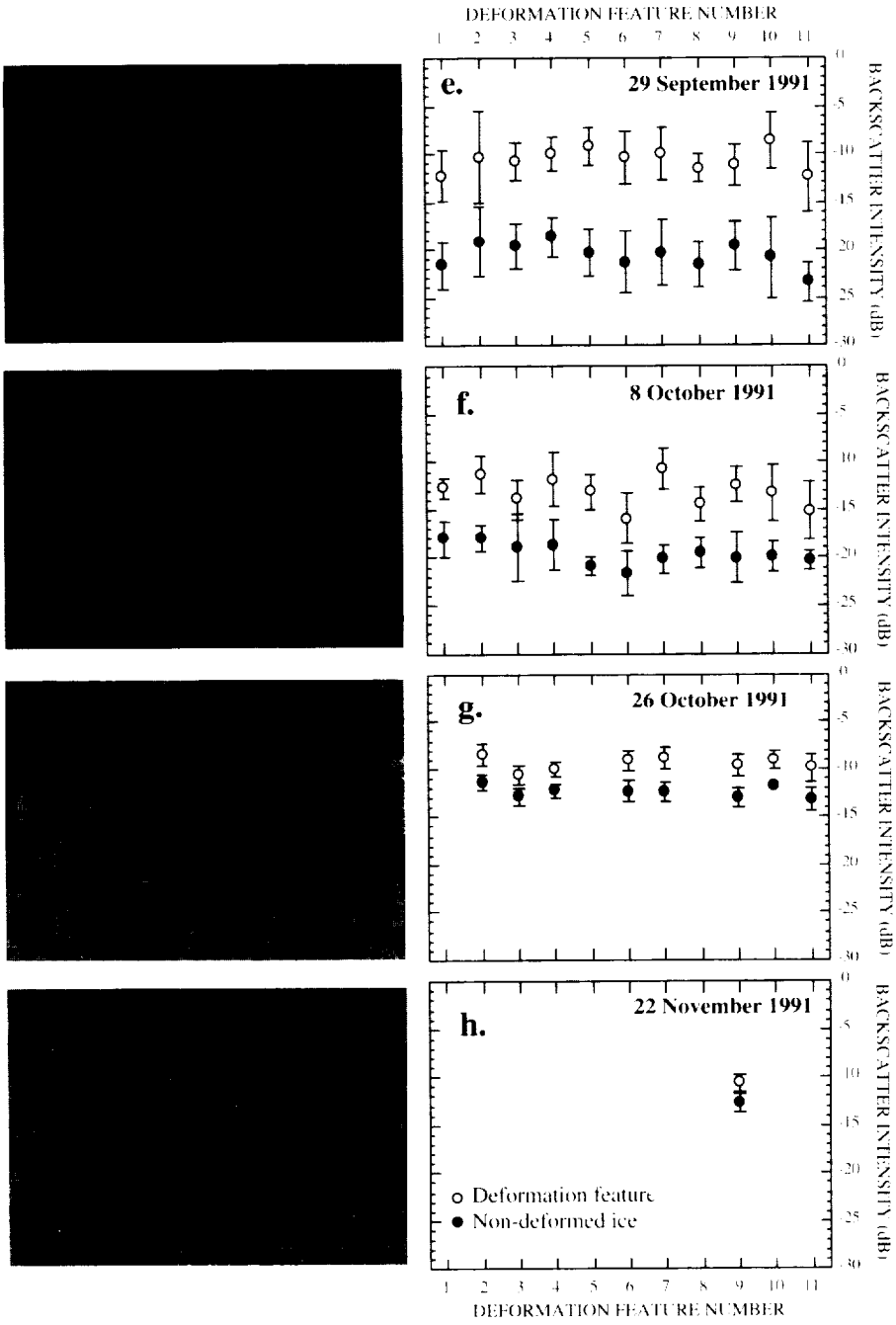

Fig. 3. Time sequence of SAR image sub-scenes of the tundra and lakes near Barrow and the differences in mean backscatter intensity between the deformation features visible on the lake-ice surfaces and the surrounding undisturbed floating ice from 29 September to 22 November 1991. The numbers in (a) identify the bright deformation features for which backscatter data are shown in (e) through (h). The sub-scenes have ground dimensions of 21.3 km by 15.3 km and are taken from ASF Standard low-resolution images with scene ID numbers: 8989200 (a); 8438200 (b); 1068200 (c); and 21213200 (d). SAR scenes are copyright ESA.

September (around Julian day 270) is typified by a sharp decrease in backscatter (Fig. 2). This is probably due to specular reflection away from the radar off the smooth upper and lower surfaces of the new, thin, continuous ice cover (Jeffries and others 1993, 1994). After initial freeze-up, backscatter values rise steadily as the ice cover thickens on all the lakes (Fig. 2).

A visual representation of the increase in backscatter during the early stages of ice growth at Barrow is shown in Figure 3. In late September, the lakes are the clearly visible dark areas, which contrast with the lighter tones of the tundra (Fig. 3a). As time progresses, backscatter from the lakes increases and the contrast between the lakes and the tundra decreases (Figs 3b and 3c). By late November, the lakes are not readily distinguishable from the surrounding land (Fig. 3d). Although the lakes typically have a dark surface during the early stages of ice growth, there are localized areas of strong returns, which are visible as narrow, bright, and generally linear features in the SAR images (Figs 3a and 3b). These are probably deformation features on the ice surface. They might be cracks related to thermal stresses generated as the thin ice cover cools, or they might be small ridging or rafting features that develop as the wind fractures and displaces the initial, thin ice cover. In either case, the strong backscatter from these features is probably due to their rough, multi-faceted, angular surfaces.

Mean and standard deviation σ° values of 11 selected deformation features and the adjacent undeformed ice are shown in Figures 3e to 3h. Soon after the initial ice formation in September, the backscatter contrast between the deformation features and the undeformed ice is high (Fig. 3e). As ice growth continues during the autumn, the contrast decreases until there is only a roughly 2 dB difference (Fig. 3h) and the deformation features 'disappear' (Fig. 3d). The final 'disappearance' of the deformation features in late November might be due to the initial development of the arrays of tubular bubbles as these shallow reservoirs are no longer able to absorb completely

the gases being expelled from the growing ice. Forward scattering off the bubbles, in combination with specular reflection off the basal ice–water interface, which shows a high contrast, could increase backscatter to a level comparable with, and subsequently greater than, the backscatter from the deformation features.

Periodic backscatter decreases and the backscatter maximum

Between late October and late January, backscatter from three of the lakes decreased sharply at different times, while backscatter increased and reached a maximum at other lakes (Fig. 2). The sharp backscatter decrease occurred at the same three lakes at different times each winter — for example, at site 11, backscatter decreased earlier in autumn 1992 than it did in autumn 1991. Those lakes where backscatter decreased are interpreted as having frozen completely to the bottom. In any given winter, the variations in the timing of the backscatter decrease reflect differences in water depth between lakes and thus the time required for the growing ice to reach the lake bottom. The differences in timing between winters probably reflect differences in the timing of initial ice formation in the autumn and subsequent ice-growth rates, which are primarily a function of air temperature and snow-cover depth. A number of Barrow lakes that froze to the bottom also had identifiable deformation features early in the ice-growth season, and these features remained visible after the ice grounded. The fact that these surface features remain visible after the ice has grounded, unlike those on floating ice that are obscured as the ice thickens but remains afloat, provides an indication of the magnitude of the signal loss in the lake bed and the relative strength of the surface scattering from the deformation features.

Those lakes where backscatter remained at a constant high level after early January are interpreted as having an ice cover that remained afloat all winter. Jeffries and others (1994) have drawn attention to the fact that backscatter from the floating ice covers reaches a maximum and saturates in January, before the ice cover and the layer of ice containing tubular bubbles have reached their maximum thickness. It has been suggested that either the layer of ice with forward-scattering tubular bubbles need only be a few centimeters thick to cause such strong backscatter, and/or there is a limit to how much backscatter the tubular bubbles can cause (Jeffries and others 1994).

The spring thaw

In May (Julian days 120–150) 1992 and 1993, unusual backscatter variations occurred (Fig. 2) at the Barrow lakes. At those lakes where backscatter was consistently high from January onwards, backscatter decreased sharply to values similar to those from lakes where the ice was aground for much of the winter. At those lakes where backscatter was consistently low, backscatter increased sharply to values similar to those from ice that had been afloat all winter. Jeffries and others (1994) first reported this unusual backscatter reversal, which occurs at the onset of air temperatures >0°C and during the subsequent spring thaw. They suggested that the reversal at these lakes was related to differences in ice surface properties and surface slope between the floating and grounded ice covers.

Changes in the snow cover also must contribute to some of the backscatter change. At temperatures <0°C, snow may be considered to be dry and thus transparent to the radar signal since there is no 'free' liquid water present (Leconte and others 1990). However, once the snow cover warms sufficiently for 'free water' to be present, the radar signal is absorbed and backscatter is reduced (Stiles and Ulaby 1980; Rott and others 1992; Hall and others 1994). This should apply whether lake-ice cover is floating or grounded, and thus backscatter should decrease at all lakes, not just from the floating ice. It should be noted that, in both 1992 and 1993, the acquisition time of all the images but one was nominally noon local time. Thus, for the spring images acquired in May and June, a moist snow cover may be considered an increasingly important factor in the radar returns. A contributing factor to the backscatter increase from the shallow lakes might be related to lake vegetation. Hall (in press) has suggested that tundra vegetation protruding through a shallow autumn snow cover causes a roughening of the snow surface relative to the C-band wavelength resulting in an increase in backscatter, especially when the vegetation is wet. In a similar fashion, vegetation protruding through a diminishing spring snow and/or ice cover on a shallow lake may cause a strong backscatter regardless of the state of the ice surface.

Spatial and year-to-year backscatter variability on the North Slope

The backscatter time series for the Alaskan North Slope lakes are quite similar from year to year, both in terms of the spatial and temporal variability and the magnitude of the values (Fig. 4). Figure 4a shows two backscatter records for a Barrow lake where the ice remained afloat all winter in 1991–92 and 1992–93. There is very little difference between the curves, except for an apparent missing backscatter minimum during freeze-up in 1992, which was due to data being unavailable between early September and early October. The backscatter records for one of the 'B' lakes that grounded in 1991–92 and 1992–93 are similar, except for the greater length of time it took for backscatter to change from high to low when the ice grounded in 1993 (Fig. 4b). Prior to grounding, maximum backscatter was close to that maintained at the Barrow lakes all winter (Fig. 4a). The timing of initial ice formation at the Barrow and 'B' lakes is coincident and clearly identified by the backscatter minimum in late September (Figs 4a and 4b). The backscatter record for a 'C' lake that was frozen to the bottom for most of the winter shows a negligible year-to-year difference between the magnitude of the backscatter values (Fig. 4c). These σ° values are similar to those from grounded ice at the 'B' lakes (Fig. 4b) and Barrow lakes (Fig. 2). These backscatter records for the Barrow, 'B', and 'C' lakes also show the onset of the spring thaw, which occurs at almost the same time each year at the same lake, and almost concurrently in any given

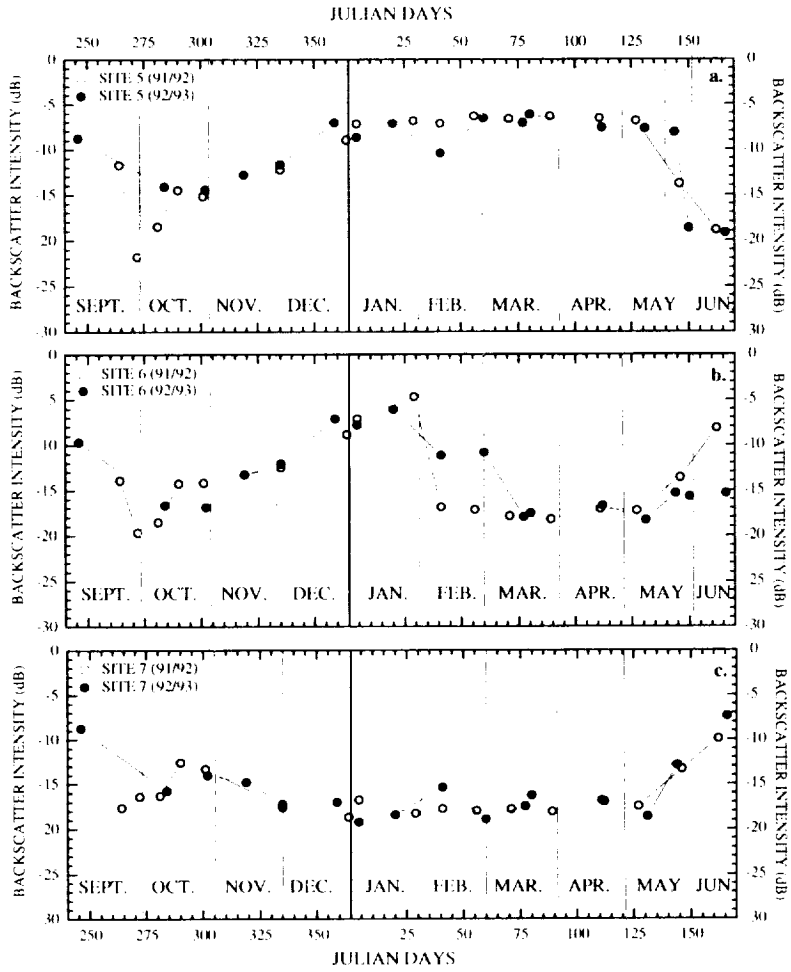

Fig. 4. Backscatter time series for the 1991–92 and 1992–93 ice seasons for selected sites on shallow Arctic lakes: a. a floating Barrow lake; b. a grounded 'B' lake; and c. a grounded 'C' lake.

year at all the lakes. The decrease in backscatter that occurs at sites where the ice is floating (Fig. 4a) and the increase that occurs where it is grounded (Figs 4b and 4c) are evidence of the onset of the spring thaw.

Shallow sub-Arctic lakes

The Naknek lakes are located adjacent to Bristol Bay in southwest Alaska, and the Kwiguk lakes are located in the Yukon River delta (Fig. 1). Each set of lakes is situated in a sub-Arctic marine environment. A backscatter time series for January to June 1992 was compiled for the Naknek lakes (a complete winter record could not be compiled because no data were available for autumn 1991). A similar backscatter time series was compiled for the Kwiguk lakes as well as a complete backscatter time series for winter 1992–93.

Naknek lakes

The backscatter record for the Naknek lakes was similar to that for the Barrow lakes, that is, there was a strong contrast in backscatter between site 5 and the other lakes from late December to late February, and at site 3 backscatter changed from strong to weak in early February (Fig. 5). As with the North Slope lakes, the interpretation of the backscatter differences is that the ice at site 5 was frozen to the lake bottom in late December, and the ice at site 3 was frozen to the bottom in February. The ice at the other lakes remained afloat all winter.

Beginning in early March, backscatter from the floating ice decreased, while that from the grounded ice increased, converging at about −11 dB in mid-March (Fig. 5). This backscatter change occurred when mean daily temperatures were above freezing for 13 of 18 days from 7 to 24 March. Consequently, there was probably an increase in the free-water content of the snow, with resultant absorption of the radar signal. The large drop in σ° values at all sites on 24 March may be the result of the cumulative effect of those above-freezing temperatures combined with precipitation on 23 and 24 March (total 17 mm water equivalent). The σ° values rose rapidly in the following few days, reaching levels similar to those immediately prior to the precipitous drop of 24 March. Mean daily temperatures below −5°C, which persisted until the end of the month, probably froze the wet snow cover, and reduced the free-water content, thereby reducing absorption of the radar signal and increasing backscatter.

The relative lack of data for April and May makes it difficult to make any detailed assessment of the processes that might have been occurring on the lakes. It appears that by early May the ice on all the lakes had melted. On 7 May, backscatter from Kvichak Bay at the northern end of Bristol Bay was very strong due to wind roughening the water surface. Wind-roughened water probably also accounts for the high radar returns from the lakes at the end of the time series (Fig. 5).

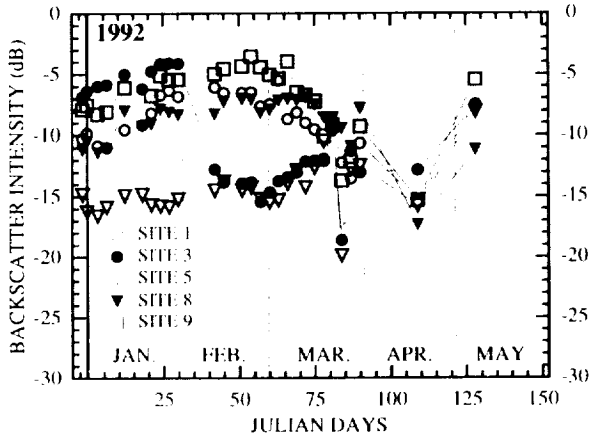

Fig. 5. Backscatter time series from December 1991 to May 1992 for sites on the shallow sub-Arctic Naknek lakes.

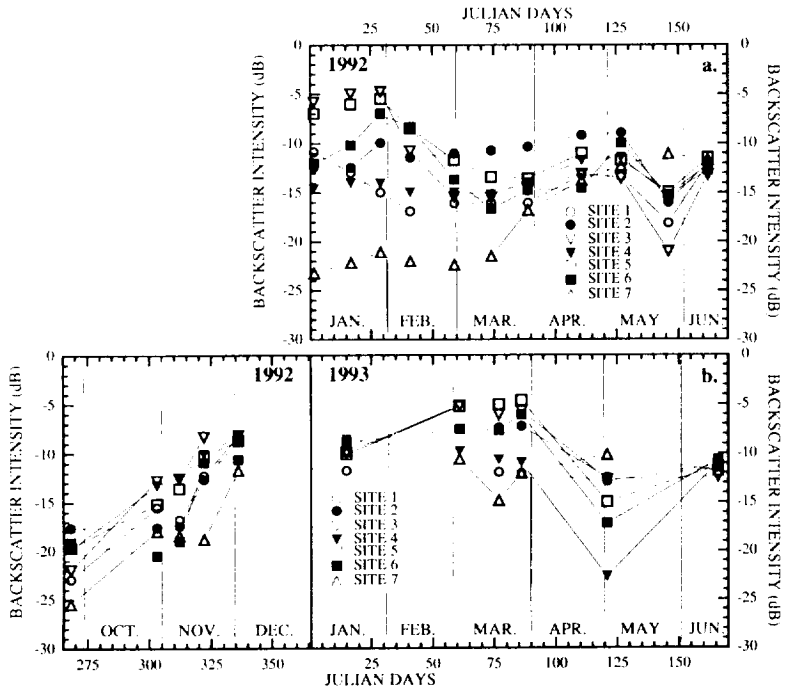

Fig. 6. Backscatter time series for the shallow sub-Arctic Kwiguk lakes from: a. January to June 1992; and b. September 1992 to June 1993.

Kwiguk lakes

The 1992–93 backscatter time series (Fig. 6b) for the Kwiguk lakes shares some features with time series for the Barrow lakes. From an initial backscatter minimum associated with freeze-up in late September, backscatter rose steadily for the remainder of the winter until a maximum was reached in March. During March, there was a short period of fairly constant maximum backscatter values before they decreased in April at the onset of the spring thaw. None of the lakes appear to have frozen to the bottom in winter 1992–93.

The winter 1992 backscatter time series (Fig. 6a) was quite different from that observed at the same time the following year (Fig. 6b). The consistently low backscatter from site 7 from early January 1992 onwards (Fig. 6a) suggests that it was grounded while the ice at the other sites was afloat. However, it should be noted that the backscatter values for site 7 were unusually low; only the initial ice cover on the shallow, Arctic lakes had a similar value (Figs 2 and 4) and it was not sustained through a period of months, as was the case at site 7. At those sites where the ice apparently remained afloat, maximum backscatter was reached on different dates in January, unlike the following year when maximum backscatter occurred in March. After maximum backscatter was reached at the Kwiguk lakes in January 1992, it decreased to minimum levels until mid-March. This might be a period when the ice was grounded on the bottom. During April 1992, a moderate backscatter increase occurred (Fig. 6a) when air temperatures at nearby Emmonak fluctuated about 0°C. This could have caused thawing and refreezing of the snow cover, creating ice layers, which are known to cause specular reflection and strongly enhanced backscatter (Mätzler and Schanda 1984). During May 1992, backscatter decreased at most sites, probably indicating the onset of the spring thaw. Only site 7 had strong backscatter at this time, perhaps due to vegetation protruding through the ice cover.

The contrast in timing of the backscatter maximum, and the apparent absence of grounding in 1993 at the Kwiguk lakes might be a reflection of winter temperature differences. In winter 1992–93, temperatures often reached almost 0°C and the weather was not as persistently cold as it had been the previous winter. Consequently, ice-growth rates might not have been as rapid and the ice did not grow as thick as it did the previous winter, and thus the ice at most sites did not ground on the bottom. A colder winter in 1991–92 is also suggested by the 1992 backscatter record, which indicates that the onset of the spring thaw occurred later in 1992 than it did in 1993; thus, the ice cover had a longer duration. It should be noted that the backscatter values from most of the grounded sites in 1992 are neither as low as those at site 7 (Fig. 6a) nor those from grounded ice at the shallow Arctic lakes (Figs 2 and 4).

Deep lakes

Tazlina Lake

Tazlina Lake is a sub-Arctic lake 22 km long located in south-central Alaska on the north side of the Chugach Mountains (Fig. 1). Although Tazlina Glacier is located at the south end of the lake, the two are not in direct contact. The depth of the lake is unknown, but, in view of its glacial origin, it is assumed to be much deeper than the shallow Arctic and sub-Arctic lakes discussed above. Backscatter was measured at 14 locations along the length of the lake (Fig. 8d) and backscatter time series were compiled for each location during winters 1991–92 and 1992–93. None of the 14 sites is believed to have grounded at any time during either winter because of the lake's depth.

A selection of the 14 backscatter time series is shown in Figure 7. Both the 1991–92 and 1992–93 records have features similar to those observed at the shallow Arctic and sub-Arctic lakes. However, there are noticeable differences between the two Tazlina Lake records. In each time series, there is a backscatter minimum in late December or early January, probably evidence of final freeze-up and the establishment of a stable ice cover. Thereafter, backscatter values increase steadily as the ice thickens. However, whereas a backscatter maximum was attained in late February 1992, in 1993 it occurred two months later, in April. One exception to the steady increase in backscatter in 1992–93 was site 3, which had strong backscatter

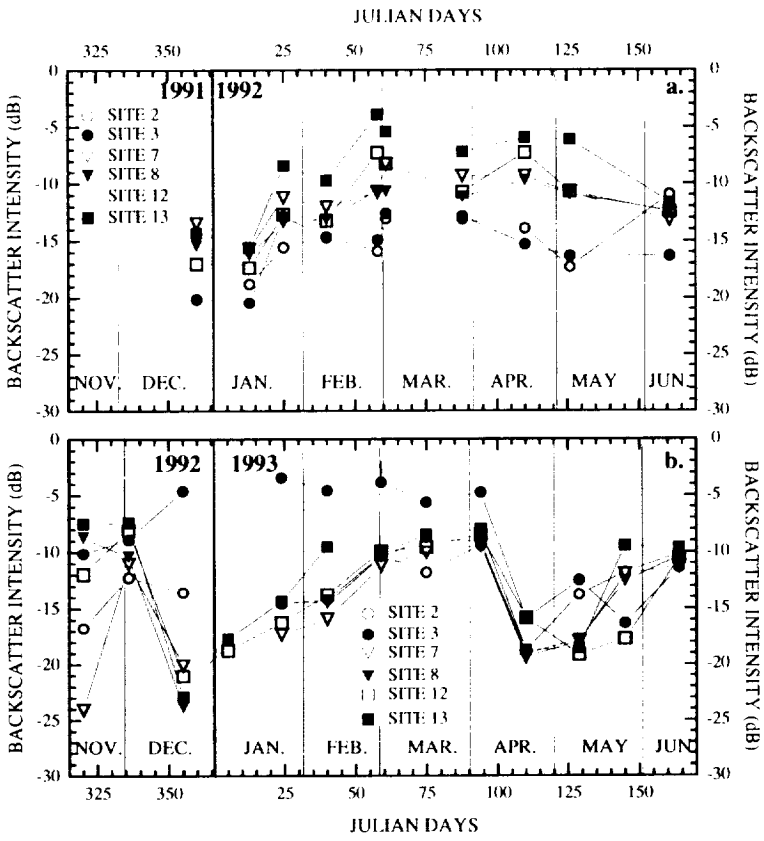

Fig. 7. Backscatter time series for selected sites on Tazlina Lake from: a. December 1991 to June 1992; and b. November 1992 to June 1993.

throughout the winter. It is located at the northern tip of the lake, where the strong backscatter is evident as a bright, roughly triangular area of ice (Fig. 8). This is probably a plug of deformed ice that was blown into this region from further south on the lake early in the ice-growth season, before a stable ice cover was established. Similar features have been observed on Canadian lakes and rivers (Leconte and Klassen 1991). During April 1993, backscatter values decreased sharply, probably as a result of the onset of the spring thaw. The timing of the onset of the spring thaw is not readily apparent in the 1992 record.

Pronounced spatial backscatter variations occurred on the ice cover at Tazlina Lake. In December 1992, apart from the strong backscatter from the deformed ice at the northern end of the lake, the ice had a fairly uniform dark tone with a network of brighter, narrow, linear features criss-crossing the lake (Fig. 8a). On 24 January 1993, this network had become more prominent (Fig. 8b) and by 9 February, it had expanded across much of the southern two-thirds of the lake (Fig. 8c). These bright features are interpreted as ice deformation features, which cause strong

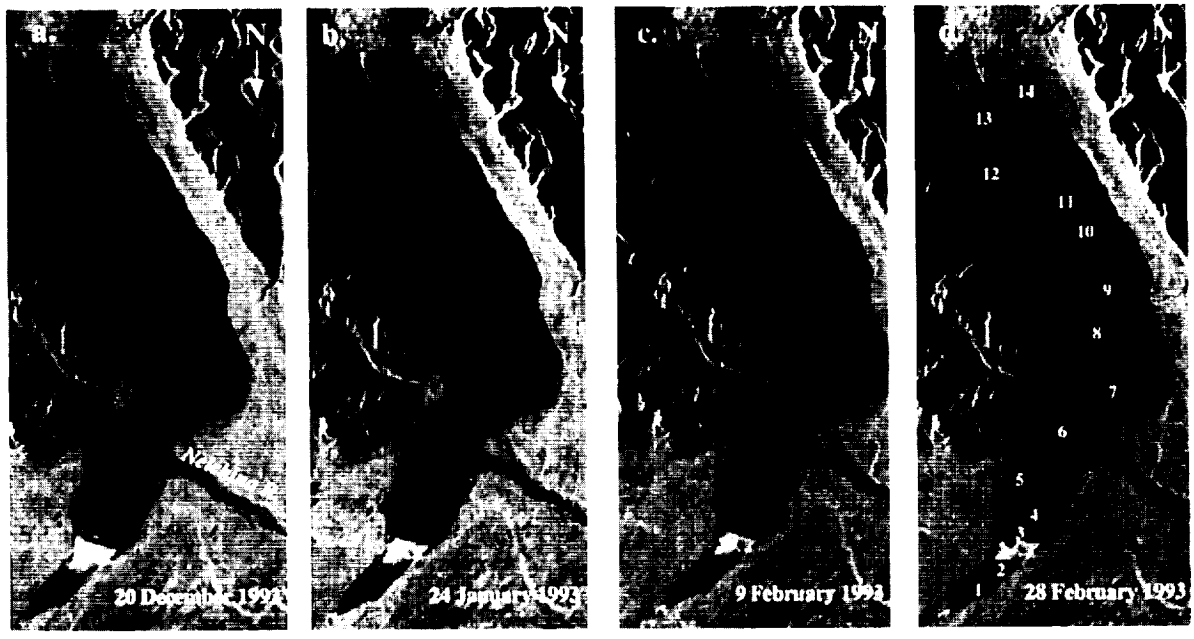

Fig. 8. Time sequence of SAR image sub-scenes of Tazlina Lake from 20 December 1992 to 28 February 1993. A network of deformation features is clearly visible on 20 December (a). These features appear to expand spatially and increase in density (b and c) until 28 February, when the lake takes on a near-uniform tone (d). The sampling sites marked in (d) were used to compile the backscatter intensity time series in Figure 7b. The sub-scenes have ground dimensions of 15.7 km by 35.4 km and are taken from ASF Standard low-resolution images with scene ID numbers 78092200 (a); 60029200 (b); 60126200 (c); and 60228200 (d). SAR scenes are copyright ESA.

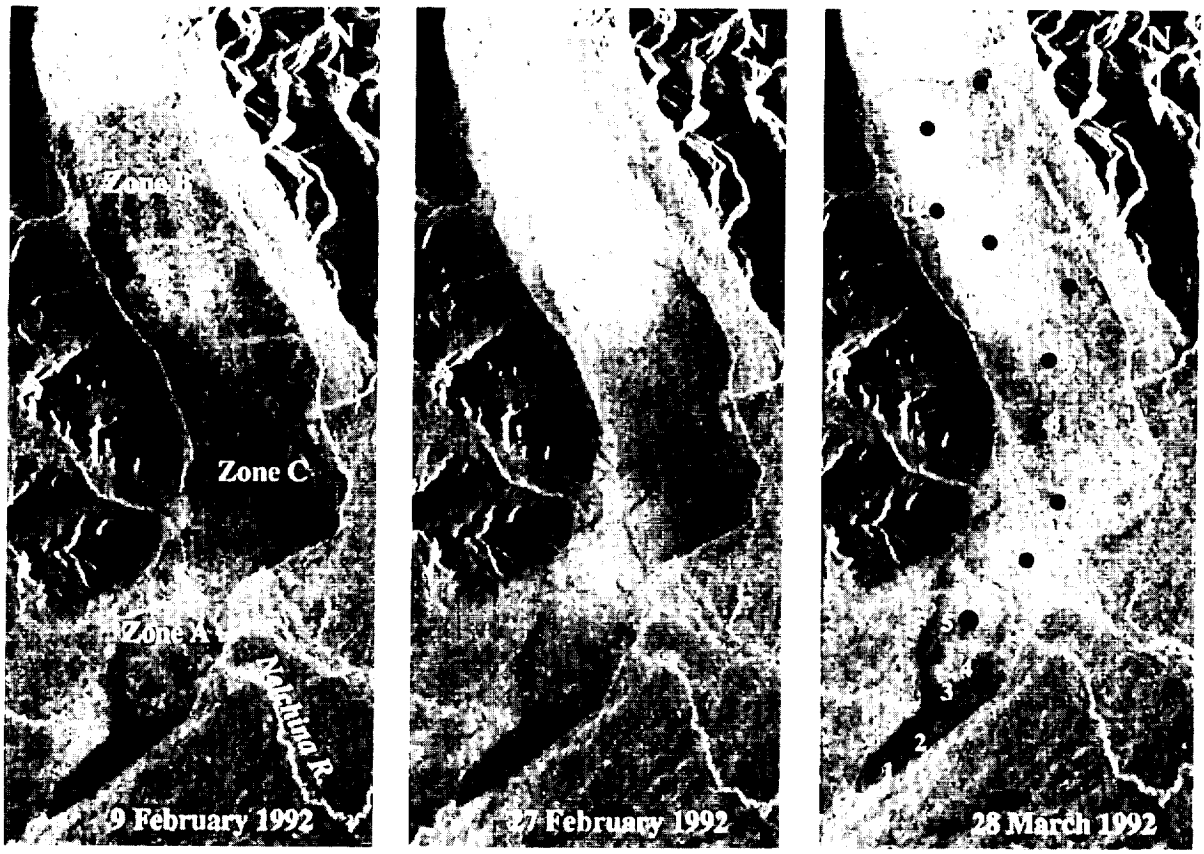

Fig. 9. Time sequence of SAR image sub-scenes of Tazlina Lake from 9 February to 28 March 1992. A network of deformation features is faintly visible on 9 February (a). Two zones of high backscatter are evident at the north and south ends of the lake (zones A and B), with a zone of lower backscatter in between (zone C). Zone B becomes very bright on 27 February (b). One month later the lake has taken on a mottled appearance (c). The sampling sites seen in (c) were used to compile the backscatter intensity time series in Figure 7a. The sub-scenes have ground dimensions of 15.7 km by 35.4 km and are from ASF Standard low-resolution images with scene IDs: 65470200 (a); 65501200 (b); and 13250200 (c). SAR scenes are copyright ESA.

backscatter, surrounded by undeformed ice with lower backscatter. The increased density of the deformation network may be due, in part, to katabatic winds that sweep down the glacier and are funnelled between the mountains on either side of the lake, thus exerting strong wind stress on the ice. This hypothesis is supported by the fact that the density of the deformation is greatest close to the glacier and decreases at the north end of the lake, where katabatic wind stress will be lower and the effects on the ice cover will be reduced. Regardless of location on the lake, the deformation features all but 'disappeared' by 28 February (Fig. 8d). The 'disappearance' of deformation features at the Barrow lakes was attributed to the initial development of the arrays of tubular bubbles in those shallow lakes. However, it is unlikely that such dense arrays of tubular bubbles develop at Tazlina Lake, if they develop at all, because the lake is deep and the gases expelled during ice growth are absorbed by this large reservoir. An alternative explanation for the 'disappearance' of deformation features is a change in air temperatures. At both Gulkana and Glenallen weather stations, 50 km east-northeast of Tazlina Lake, daily maximum temperatures >0°C occurred on 26–28 February. Similar temperatures at Tazlina Lake could have changed the nature of the snow cover sufficiently to cause higher and near-uniform backscatter from the lake on 28 February.

The spatial variability of backscatter in winter 1991–92 differed sharply from that in 1992–93. One significant difference was that any deformation features that existed in 1992 (Fig. 9a) were not as well defined as in 1993 (Fig. 8c). This might be an indication that the ice was less deformed in 1992 than in 1993, or it might indicate that other factors, such as a modified snow cover, played a stronger role in affecting backscatter in 1992. In winter 1992, there was strong zonation of backscatter across the lake at any given time; zones A, B, and C had different backscatter characteristics that gave the lake a non-uniform appearance (Fig. 9a). The contrast between the strong backscatter from zone B at the south end of the lake compared to the lower backscatter from zone C in the central part of the lake was particularly striking (Fig. 9b). Similar backscatter variability has been observed at alpine lakes in Montana, where it has been attributed to localized flooding of the snow cover and snow-ice formation (Hall and others 1994). Jeffries and others (1994) have drawn attention to the fact that flooding of the base of the snow

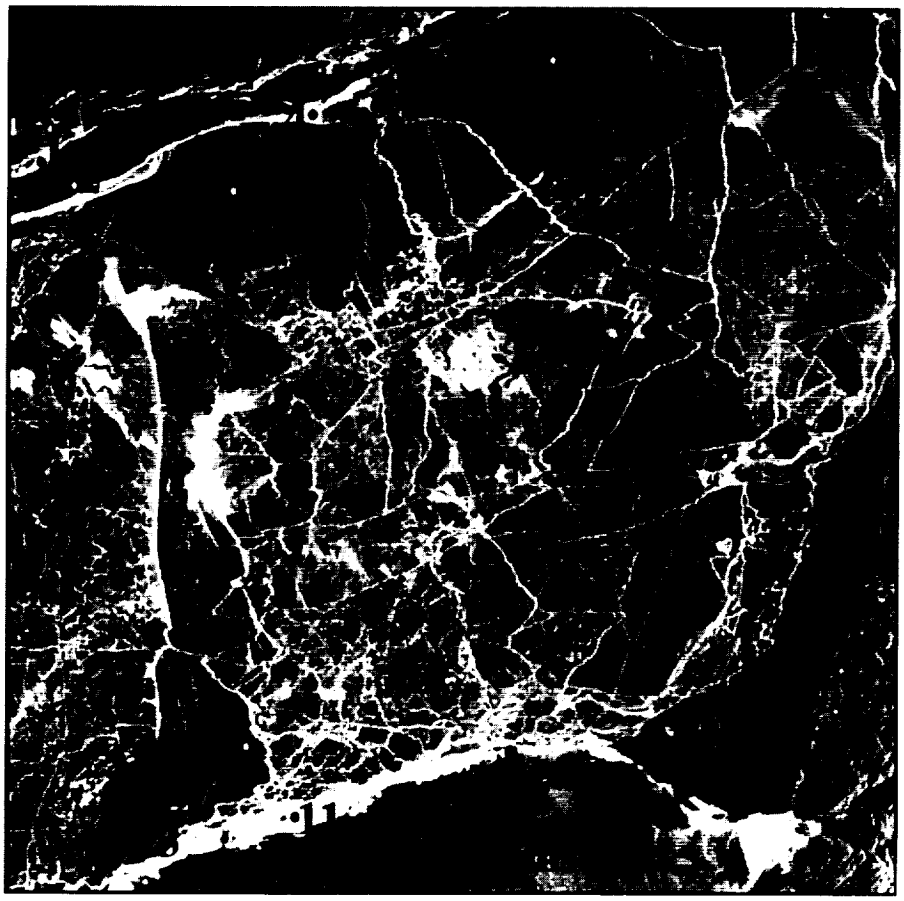

Fig. 10. The extensive network of deformation features in McTavish Arm, the northeastern section of Great Bear Lake, is clearly visible in this ERS-1 SAR data acquired on 1 January 1992 (ASF image ID 14507200). The sub-scene has ground dimensions of 71.6 km by 71.3 km. This network becomes established in December and persists until the spring melt. The numbered locations are the sampling sites used to created the backscatter time series in Figure 11. SAR scene is copyright ESA.

cover is common on Antarctic sea ice, and that strong backscatter has been reported from flooded ice due to the strong dielectric contrast between the upper layer of dry snow and the underlying slush (Lytle and others 1990). A similar mechanism might cause strong backscatter from flooded lake ice. Once the slush freezes, strong backscatter might continue because of the bubbly nature of snow-ice. Regardless of the specific causes of the backscatter variability in Figure 9, it seems likely that backscatter in each zone was controlled by different factors, otherwise the lake might be expected to have a more uniform appearance, such as that observed in 1993 (Fig. 8d).

Great Bear Lake

Great Bear Lake is a deep Arctic lake located in the extreme northwest of the Canadian Northwest Territories (Fig. 1). Backscatter time series were compiled for 13 sites in McTavish Arm, located in the northeast region of Great Bear Lake. The SAR image of McTavish Arm (Fig. 10) shows a dense network of deformation features. The strong backscatter from these features is exemplified by sites 1 and 11, located along the northern and southern shores of the arm, respectively. Backscatter from the ice adjacent to the deformation features has a much darker appearance, with variable grey tones. A selection of the backscatter time series (Fig. 11) shows a pattern similar to that observed at the other lakes, that is, after the establishment of a stable ice cover, backscatter rises steadily and in early January reaches maximum values, which are maintained for the rest of the winter (Fig. 11). The time series does not show the onset of the spring thaw because data were not available for McTavish Arm after early May. By 27 May, deformation features were barely visible in SAR images of the lake-ice cover immediately west of McTavish Arm, suggesting that the spring thaw had begun.

The SAR images used to investigate lake-ice processes on Great Bear Lake showed that a stable ice cover was not established until late December. In subsequent images, the position of the deformation features remained the same, an indication of the stability of the ice cover once it had been established. Prior to late December, ice was forming on the lake, but it was subject to wind stress and displacement. The network of deformation features reflects this initial instability. The presence of ice of different ages and thicknesses, resulting from the convergence and divergence early in the ice-growth season, probably accounts for the variability in backscatter from the darker-toned ice adjacent to the deformation features.

Discussion

Mean σ° values for grounded ice and floating ice were calculated for all categories of lakes (Fig. 12). The shallow Arctic lakes have fairly consistent mean backscatter values for both floating and grounded ice, from site to site and year to year, with a mean σ° value of -6.4 ± 0.5 dB for all

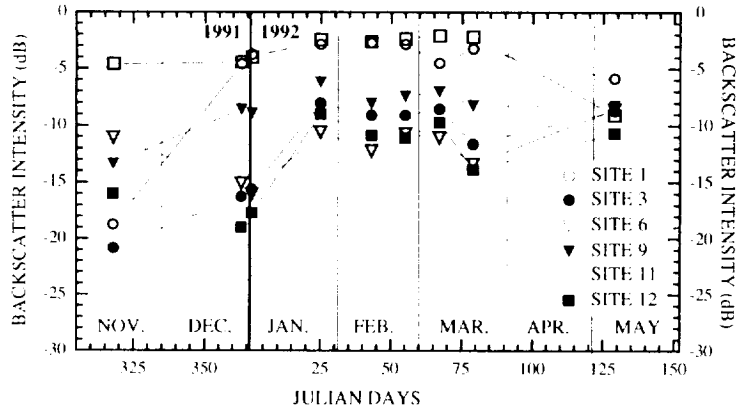

Fig. 11. Backscatter time series for selected sites on the eastern section of Great Bear Lake from November 1991 to May 1992. Note that this time series does not extend to the onset of melting due to lack of data.

floating ice sites and -16.2 ± 1.1 dB for all grounded ice sites. The similarities in the σ° values between sites and between years is probably due to the fact that during typical winters on the North Slope, temperatures remain continuously below freezing between freeze-up and spring, and only 'dry' snow falls; thus, the ice surface and the resultant backscatter are not dramatically altered by thawing and freezing cycles, or by the introduction of liquid water.

The floating ice on the shallow sub-Arctic lakes has a mean σ° value (-6.5 ± 0.4 dB) similar to that of floating ice on the shallow Arctic lakes (Fig. 12). This is most likely because the ice on both types of lakes has similar characteristics, due to gas supersaturation of the shallow water and tubular bubble development, and the resultant effects on backscatter. However, the mean σ° value of grounded ice on sub-Arctic lakes is -13.2 ± 1.5 dB, which is 3 dB higher than the value for grounded ice at the Arctic lakes (Fig. 12). As noted previously, backscatter from the grounded zones of the shallow Arctic lakes is low because of the low dielectric discontinuity between the ice and lake sediment; consequently, most of the radar signal is simply absorbed in the lake sediments. In late April 1992 and early May 1993, when observations and measurements were made on the Barrow lakes in conjunction with ERS-1 SAR data acquisition (Jeffries and others 1993, 1994; Wakayabashi and others 1993a), the sediment below grounded ice was found to be dry and frozen. This can be explained by the continued transfer of energy through the ice to the surface after the ice grounds. In this case, the energy source is the wet sediment rather than the lake water. In time, during the persistently cold, dry winter, sufficient energy will be transferred through the grounded ice to freeze the sediments and desiccate them, perhaps by ice segregation and development of ice lenses within the sediment.

In the sub-Arctic areas, winter temperatures are more variable and not as persistently cold as on the North Slope. Consequently, once the lake ice grounds on the bottom, the rate and amount of energy transferred upwards from the sediments might be lower than occurs at the Arctic lakes, and the sediments might become neither as dry nor as completely frozen as the North Slope lake sediments. If there is still some free water in the soil, the dielectric discontinuity between it and the grounded ice would be higher and the radar return from the interface between the base of the lake ice and the partially frozen sediment might also be higher. Results of backscatter modelling of snow-covered terrain indicate that: 1. as air temperatures decrease, backscatter decreases as a consequence of a reduc-

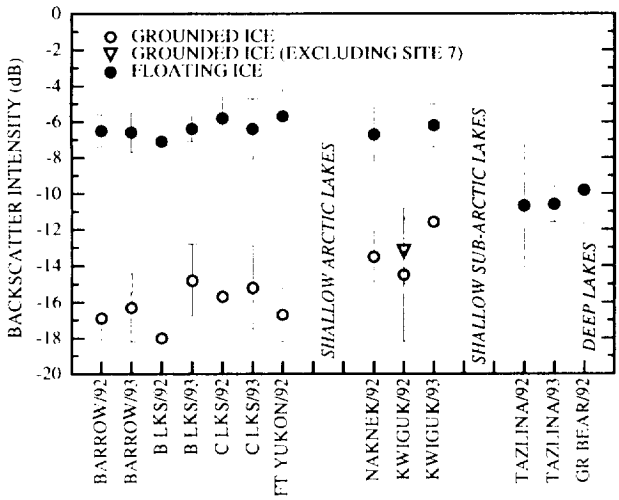

Fig. 12. Mean backscatter values for grounded and floating ice covers on the Arctic and sub- Arctic shallow lakes and on the deep lakes.

tion in the water content of the soil; and 2. the dynamic range of the backscatter varies between soil types as a consequence of differing unfrozen water content (Leconte 1993). There is an analogy between the snow-covered terrain and the ice-covered lake sediment, and it may be that unfrozen, or partially frozen, sediments overlain by grounded lake ice have similar effects on radar backscatter.

Excluding deformation features, which have very high backscatter, the overall mean backscatter from the ice on the deep lakes is -10.4 ± 0.5 dB. This is a full 4 dB lower than backscatter from floating ice on the shallow lakes (Fig. 12). Whereas tubular bubbles develop in the ice on the shallow lakes, they are most likely absent from the ice on the deep lakes where most, if not all, gases expelled during ice growth are absorbed in these deep reservoirs. The 4 dB difference between the shallow and deep lake-ice covers is probably a measure of the effectiveness of the tubular bubbles as forward scatterers, which enhance the return from the basal ice–water interface.

As the ice thickens on the deep lakes, backscatter increases during the winter and often reaches a maximum, which is maintained at nearly constant values until the spring thaw (Figs 7a and 11). The same backscatter increase occurs in the early stages of ice growth on the shallow lakes (Figs 2 and 4). The ice-core records for the Barrow lakes show clear ice overlying ice containing many tubular bubbles (Jeffries and others 1993, 1994; Wakayabashi and others 1993a), indicating that, prior to the initial development of the tubular bubbles, the lakes were able to absorb most if not all of the gases expelled during ice growth. Swift and others (1980) and Hall and others (1994) have reported stronger backscatter from thick ice than from thin ice on deep lakes. The increase in backscatter that occurs concurrent with the increase in ice thickness at the shallow Arctic lakes has been reproduced by a numerical model of lake-ice backscatter (Wakayabashi and others 1993a, 1993b). However, a satisfactory explanation for this phenomenon remains to be found.

Also unexplained is the maintenance of a backscatter maximum that occurs at the shallow lakes with tubular bubble layers and at the deep lakes, where presumably few if any tubular bubbles are present. As noted, either the layer of ice with forward-scattering tubular bubbles need only be a few centimeters thick to cause such strong backscatter, and/or there is a limit to how much backscatter the tubular bubbles can cause (Jeffries and others 1994). Similarly, there might be an upper limit to the amount of backscatter that can occur from clear, inclusion-free freshwater ice.

Conclusions

This survey of radiometrically calibrated ERS-1 SAR images of sub-Arctic and Arctic lakes has shown that a variety of lake-ice processes can be observed and that significant changes in backscatter occur during the course of lake-ice growth and decay. Regardless of lake location and water depth, SAR can provide data on the timing of freeze-up and the onset of the spring thaw.

Spatial and temporal changes in backscatter are the most constant and predictable at the shallow lakes on the North Slope of Alaska, most likely due to the persistently cold winters and the absence of detrimental climatic factors that complicate the interpretation of backscatter in relation to lake-ice processes and growth history. Similar ice processes and growth history occur at the shallow sub-Arctic lakes, but there is greater backscatter variability in any given growth season and between growth seasons. This can be attributed to the more variable winter climate of the sub-Arctic marine locations. Ice processes, growth history and backscatter at the large, deep lakes, can also vary significantly, both at any one time, and from year to year.

The predictability of backscatter in relation to ice processes and growth history at the shallow Arctic lakes suggests that they would be promising sites for long-term monitoring and the detection of changes related to global warming and its effects on the polar regions. Since winters are persistently cold, a small climatic perturbation ought to have noticeable consequences. For example, a delay in the onset of ice growth in autumn coupled with warmer winter temperatures might be reflected in a thinner ice cover and delays in the timing of and a reduction in the area of ice freezing to the bottom of the lakes. An analogous situation might be occurring today at the Kwiguk lakes on the Yukon delta. There, the backscatter records suggested that the ice grounded on the bottom of the lakes one winter, but did not ground at all the next winter due to differences in winter temperatures. Long-term monitoring of winter climate in relation to whether lake ice grounds or not, and the duration of grounding when it does occur, could be done with SAR.

In order fully to exploit the potential of SAR for studies of lake-ice processes and history in relation to environmental change, further research on the relationships between lake ice and backscatter variability is still required. A number of backscatter phenomena remain to be satisfactorily explained with respect to ice processes and growth history. These include:

1. identification of the minimum thickness of an ice layer with tubular bubbles and the minimum thickness of clear ice required to produce a backscatter maximum;
2. identification of the causes of the limits on backscatter from clear ice and ice containing tubular bubbles;
3. determination of whether tubular bubbles nucleate in ice on deep lakes and in what quantities;
4. determination of the effects of variable water content of lake sediment on backscatter from ice grounded on those sediments;
5. quantification of the effects of variable snow-cover properties on backscatter from the underlying ice, including the consequences of flooding and subsequent snow-ice formation; and

6. identification of the causes of the backscatter reversals that occur with particular strength during the spring thaw at the Barrow lakes.

Acknowledgements

This work was supported by NASA Polar Program Grant NAG5-1731. Dr Tony Freeman of the Jet Propulsion Laboratory in Pasadena, California, kindly made available the MacSigma-0 software. The Alaska SAR Facility provided SAR images in a timely fashion. ERS-1 SAR scenes are copyright ESA.

References

Chapman, W.E., and J.E. Walsh. 1993. Recent variations of sea ice and air temperature in high latitudes. *Bulletin of the American Meteorological Society* 74: 33–47.

Elachi, C., M.L. Bryan, and W.F. Weeks. 1976. Imaging radar observations of frozen Arctic lakes. *Remote Sensing of Environment* 5: 169–175.

Hall, D.K. In press. Remote sensing of snow and ice using imaging radar. In: Ryerson, R. (editor). *Manual of remote sensing.* 3rd edition. Bethesda, MD: American Society of Photogrammetry and Remote Sensing.

Hall, D.K., D.B. Fagre, F. Klasner, G. Linebaugh, and G.E. Liston. 1994. Analysis of ERS-1 data of frozen lakes in northern Montana and implications for climate studies. *Journal of Geophysical Research* 99 (C11): 22,473–22,482.

Jeffries, M.O., H. Wakabayashi, and W.F. Weeks. 1993. ERS–1 SAR backscatter changes associated with ice growing on shallow lakes in Arctic Alaska. In: *Better understanding of Earth environment: proceedings of IGARSS '93 symposium, Tokyo, Japan, 18–21 August 1993.* Piscataway, NJ: The Institute of Electrical and Electronics Engineers: IV, 2001–2004.

Jeffries, M.O., K. Morris, W.F. Weeks, and H. Wakayabashi. 1994. Structural and stratigraphic features and ERS-1 SAR backscatter characteristics of ice growing on lakes in NW Alaska, winter 1991–92. *Journal of Geophysical Research* 99 (C11): 22,459–22,471.

Leconte, R. 1993. Modelling the interaction between microwaves and a snow/soil system. In: Barry, R.G., B.E. Goodison, and E.F. LeDrew (editors). *Snow watch '92: detection strategies for snow and ice.* Boulder, Colorado: World Data Center A for Glaciology (Report GD-25): 188–203

Leconte, R., and P.D. Klassen. 1991. Lake and river ice investigations in northern Manitoba using airborne SAR imagery. *Arctic* 44 (Supplement 1): 153–163.

Leconte, R., T. Carroll, and P. Tang. 1990. Preliminary investigations on monitoring the snow water equivalent using synthetic aperture radar. In: Ferrick, M. *Proceedings of the forty-seventh annual Eastern Snow Conference, 7–8 June 1990, Bangor, Maine.* CRREL Special Report 90-44: 73–86.

Lytle, V.I., K.C. Jezek, S. Gogineni, R.K. Moore, and S.F. Ackley. 1990. Radar backscatter measurements during the Winter Weddell Gyre Study. *Antarctic Journal of the United States* 25 (5): 123–125.

Manabe, S., M.J. Spelma, and R.J. Stouffer. 1992. Transient responses of a coupled ocean–atmosphere model to gradual changes of atmospheric CO_2, II, seasonal response. *Journal of Climatology* 5 (2): 105–126.

Mätzler, C., and E. Schanda. 1984. Snow mapping with active microwave sensors. *International Journal of Remote Sensing* 5 (2): 409–422.

Mellor, J. 1982. Bathymetry of Alaskan Arctic lakes: a key to resource inventory with remote sensing methods. Unpublished PhD thesis. Institute of Marine Science, University of Alaska.

Palecki, M.A., R.G. Barry, and F. Tramoni. 1985. Lake freeze-up and break-up records as a temperature indicator for detecting climate change. In: *Extended abstracts, third conference on climatic variations.* Los Angeles: American Meteorological Association: 29–30.

Palecki, M.A., and R.G. Barry. 1986. Freeze-up and break-up of lakes as an index of temperature changes during the transition seasons: a case study in Finland. *Journal of Climate and Applied Meteorology* 25 (7): 893–902.

Rott, H., R.E. Davis, and J. Dozier. 1992. Polarimetric and multifrequency SAR signatures of wet snow. In: Williamson, R. (editor). *International space year: space remote sensing: proceedings of IGARSS '92 symposium, Houston, Texas, May 26–29, 1992.* Piscataway, NJ: The Institute of Electrical and Electronics Engineers: III, 1658–1660.

Schindler, D.W., K.G. Beaty, E.J. Fee, D.R. Cruikshank, E.R. DeBruyn, D.L. Findlay, G.A. Linsey, J.A. Shearer, M.P. Stainton, and M.A. Turner. 1990. Effects of climatic warming on lakes of the central boreal forest. *Science* 250: 967–970.

Sellmann, P.V., W.F. Weeks, and W.J. Campbell. 1975a. *Use of sidelooking airborne radar to determine lake depth on the Alaskan North Slope.* Hanover, New Hampshire: US Army Cold Regions Research and Engineering Laboratory (CRREL Special Report 230).

Sellman, P.V., J. Brown, R.I. Lewellen, H. McKim, and C. Merry. 1975b. *The classification and geomorphic implications of thaw lakes on the Arctic Coastal Plain, Alaska.* Hanover, New Hampshire: US Army Cold Regions Research and Engineering Laboratory (CRREL Special Report 344).

Stiles, W.H., and F.T. Ulaby. 1980. The active and passive microwave response to snow parameters: 1. wetness. *Journal of Geophysical Research* 85 (C2): 1037–1044.

Swift, C.T., W.L. Jones, R.F. Harrington, J.C. Fedors, R.H. Couch, and B.L. Jackson. 1980. Microwave radar and radiometric remote sensing measurements of lake ice. *Geophysical Research Letters* 7: 243–246.

Wakabayashi, H., M.O. Jeffries, and W.F. Weeks. 1993a. C-band backscatter from ice on shallow tundra lakes: observations and modelling. In: Kaldeich, B. (editor). *Proceedings of the first ERS-1 symposium; space at the service of our environment, 4–6 November 1992, Cannes, France.* Paris: European Space Agency (ESA SP-359): 333–337.

Wakabayashi, H., W.F. Weeks, and M.O. Jeffries. 1993b. A C–band backscatter model for lake ice in Alaska. In: *Better understanding of Earth environment: proceedings of IGARSS '93 symposium, Tokyo, Japan, 18–21 August 1993.* Piscataway, NJ: The Institute of Electrical and Electronics Engineers: III, 1264–1266.

Weeks, W.F., P.V. Sellmann, and W.J. Campbell. 1977. Interesting features of radar imagery of ice-covered North Slope lakes. *Journal of Glaciology* 18 (78): 129–136.

Weeks, W.F., A.G. Fountain, M.L. Bryan, and C. Elachi. 1978. Differences in radar returns from ice-covered North Slope lakes. *Journal of Geophysical Research* 83 (C8): 4069–4073.

Weeks, W.F., A.J. Gow, and R.J. Schertler. 1981. *Ground-truth observations of ice-cover on North Slope lakes imaged by radar.* Hanover, New Hampshire: US Army Cold Regions Research and Engineering Laboratory (CRREL Research Report 81-19).

The accuracy of references in the text and in this list is the responsibility of the authors, to whom queries should be addressed.